STUDIES OF JET PROPERTIES AT THE TEVATRON

Mario Martínez
Instituto de Física de Altas Energías
Universidad Autónoma de Barcelona
E-80193 Bellaterra (Barcelona) Spain
(*On behalf of the CDF Collaboration)*

Abstract

In this contribution, a number of new QCD results on jet production from the CDF and DØ experiments in Run II are discussed in detail.

1 Introduction

The Run II at the Tevatron will define a new level of precision for QCD studies in hadron collisions. Both collider experiments, CDF and D0, expect to collect up to 8 fb^{-1} of data in this new run period. The increase in instantaneous luminosity, center-of-mass energy (from 1.8 TeV to 2 TeV) and the improved acceptance of the detectors will allow stringent tests of the Standard Model (SM) predictions in extended regions of jet transverse momentum, P_T^{jet}, and jet rapidity, Y^{jet}. The hadronic final states in hadron-hadron collisions are characterized by the presence of soft contributions (the so-called *underlying event*) from initial-state gluon radiation and mutiple parton interactions between remnants, in addition to the jets of hadrons originated by the hard interaction. A proper comparison with pQCD predictions at the parton level requires an adequate modeling of these soft contributions which become important at low $\mathrm{P_T^{jet}}$. In this letter, a review of some of the most important QCD results from Run II is presented.

2 Inclusive Jet Production at the Tevatron

The measurement of the inclusive jet production cross section for central jets constitutes one of the pillars of the jet physics program at the Tevatron. It provides a stringent test of perturbative QCD predictions over almost nine orders of magnitude and probes distances up to $\sim 10^{-19}$m. Thanks to the increase in the center-of-mass energy in Run II the jet production rate has been multiplied (by a factor of five for jets with $P_T^{\mathrm{jet}} > 600$ GeV) and the first measurements have already extended the P_T^{jet} coverage by 150 GeV compared to Run I. In addition, both CDF and D0 experiments explore new jet algorithms following the theoretical work that indicates that the cone-based jet algorithm employed in Run I is not infrared safe and compromises a future meanful comparison with pQCD calculations at NNLO. Figure 1 shows the measured inclusive jet cross section by CDF using the longitudinally invariant K_T algorithm [1)] and based on the first 145 pb^{-1} of Run II data. Measurements have been performed using values for the D parameter in the K_T expression,

$$K_{ij} = \min(\mathrm{p_{T,i}^2}, \mathrm{p_{T,j}^2}) \cdot \frac{(\mathrm{y_i} - \mathrm{y_j})^2 + (\phi_\mathrm{i} - \phi_\mathrm{j})^2}{\mathrm{D}} \quad , \tag{1}$$

equal to 0.5, 0.7 and 1.0. The measurements are compared to pQCD NLO calculations [2)] using CTEQ6 [3)] parton density functions in the proton and antiproton and the renormalization and factorization scales set to $p_T^{\mathrm{max}}/2$. The measured cross section is reasonably well described by the predictions for $P_T^{\mathrm{jet}} > 150$ GeV within the present uncertainties. The systematic errors on

Figure 1: *The measured inclusive jet cross section compared to pQCD NLO predictions. Jets are seached for using the longitudinally invariant K_T algorithm.*

the data are dominated by the uncertainty on the jet energy scale determination while the theoretical predictions suffer from our limited knowledge of the gluon distribution at high x. At lower $P_T^{\rm jet}$, the data is systematically above the predictions and the effect increases as D increases (see Figure 2). This indicates the presence of soft-gluon contributions and fragmentation effects that have not been taken into account yet.

Figure 2: *Ratio between the measured inclusive jet cross section and the pQCD NLO predictions using the K_T algorithm with D=0.5 and D=0.7, respectively.*

Figure 3 shows the measured inclusive jet cross section by D0 based on the first 143pb^{-1} of Run II data. The new midpoint [4] jet algorithm has been used with a cone size R=0.7. This algorithm constitutes an improved version of the cone-based algorithm used in Run I and it is shown to be infrared safe when used in fixed-order parton-level calculations. The data is in good agreement

with the pQCD NLO predictions using CTEQ6 parton density functions and $R_{\rm sep} = 1.3$. However, the measurement is dominated by a relatively large uncertainty on the absolute jet energy scale. Figure 4 shows the measured

Figure 3: *The measured inclusive jet cross section by D0 compared to pQCD NLO predictions. Jets are seached for using the midpoint jet algorithm.*

cross section by D0 as a function of the dijet invariant mass in dijet production of central jets. This measurement is particularly sensitive to the presence of narrow resonances decaying into jets of hadrons up to masses of 1.3 TeV. The data is well described by pQCD NLO predictions.

Figure 4: *The measured inclusive dijet cross section by D0 as a function of the dijet mass compared to pQCD NLO predictions.*

Nowadays, the Tevatron high-$P_T^{\rm jet}$ jet data is used, together with prompt-photon data from fixed target experiments, to constrain the gluon distribution at high-x. Jet measurements at large rapidities are important because they

constrain the gluon density in a region in $P_T^{\rm jet}$ where no effect from new physics is expected. The D0 experiment has already extended the jet cross section measurements to the forward region for jets with $|y| < 2.4$ (see Figure 5). At

Figure 5: *(Left) measured inclusive jet cross section by D0 in different regions of rapitidy compared to pQCD NLO predictions.(Right) ratio between the measurements and the pQCD NLO predictions for jets with* $2.0 < |y| < 2.4$.

the moment, the results are affected by large systematic errors. In the near future the experiments will highly reduce their uncertainties and precise cross section measurements will allow to further constrain the gluon distribution and thus enhance their sensitivity to new physics at very high $P_T^{\rm jet}$.

3 Study of the Underlying Event

As mentioned in previous section, the hadronic final states at the Tevatron are characterized by the presence of soft underlying emissions, usually denoted as *underlying event*, in addition to highly energetic jets coming from the hard interaction. The underlying event contains contributions from initial- and final-state soft gluon radiation, secondary semi-hard partonic interactions and interactions between the proton and anti-proton remnants that cannot be described by perturbation theory. These processes must be approximately modeled using Monte Carlo programs tuned to describe the data. The jet energies measured in the detector contain an underlying event contribution that has to be subtracted in order to compare the measurements to pQCD predictions. Hence, a proper understanding of this underlying event contribution is crucial to reach the desired precision in the measured jet cross sections. In the analysis presented here, the underlying event in dijet production has been studied by looking at regions well separated from the leading jets, where the underlying event contribution is expected to dominate the observed hadronic

activity. Jets have been reconstructed using tracks with $p_T^{\rm track} > 0.5$ GeV and $|\eta^{\rm track}| < 1$ and a cone algorithm with R=0.7. The ϕ space around the leading jet is divided in three regions: *towards*, *away* and *transverse* (see Figure 6-left), and the transverse region is assumed to reflect the underlying event contribution. Figure 6-right shows the average track density in the transverse region

Figure 6: *(Left) Scheme of the different ϕ regions defined around the leading jet. (Right) Measured average track density in the transverse region as a function of the $E_T^{\rm jet}$ of the leading jet. The measurements are compared to different Monte Carlo models.*

as a function of $E_T^{\rm jet}$ of the leading jet for the dijet inclusive sample and for events where the leading jets are forced to be back-to-back in ϕ, in order to further reduce extra hard-gluon radiation. The observed plateau indicates that the underlying event activity is, to a large extend, independent from the hard interaction. The measurements have been compared to the predictions from PYTHIA [5] and HERWIG [6] Monte Carlo programs including leading-order QCD matrix elements plus initial and final parton showers. The PYTHIA samples have been created using a special tuned set of parameters, denoted as PYTHIA-Tune A, which includes an enhanced contribution from initial-state soft gluon radiation and a tuned set of parameter to control secondary parton interactions. It was determined as a result of similar studies of the underlying event performed using CDF Run I data [7]. PYTHIA-Tune A describes the hadronic activity in transverse region while HERWIG underestimates the radiation at low $E_T^{\rm jet}$. Similar measurements in Z+jet(s) events would allow to explore the univesality of the underlying event contribution in events with a very different colour configuration in the final state.

4 Jet Shapes

The internal structure of jets is dominated by multi-gluon emissions from the primary final-state parton. It is sensitive to the relative quark- and gluon-jet fraction and receives contributions from soft-gluon initial-state radiation and beam remnant-remnant interactions. The study of jet shapes at the Tevatron provides a stringent test of QCD predictions and tests the validity of the models for parton cascades and soft-gluon emissions in hadron-hadron collisions. The CDF experiment has presented results on jet shapes for central jets with transverse momentum in the region 37 GeV $< P_T^{\rm jet} <$ 380 GeV, where jets are searched for using the midpoint[1] algorithm and a cone size $R = 0.7$. The integrated jet shape, $\Psi(r)$, is defined as the average fraction of the jet transverse momentum that lies inside a cone of radius r concentric to the jet cone:

$$\Psi(r) = \frac{1}{\mathrm{N_{jet}}} \sum_{\mathrm{jets}} \frac{P_T(0,r)}{P_T(0,R)}, \quad 0 \leq r \leq R \tag{2}$$

where $N_{\rm jet}$ denotes the number of jets. The measured jet shapes have been compared to the predictions from PYTHIA-Tune A and HERWIG Monte Carlo programs.

Figure 7: *The measured integrated jet shape compared to different Monte Carlo predictions.*

In addition, two different PYTHIA samples have been used with default parameters and with and without the contribution from multiple parton interactions (MPI) between proton and antiproton remnants, the latter denoted as PYTHIA-(no MPI), to illustrate the importance of a proper modeling of soft-gluon radiation in describing the measured jet shapes. Figure 7(left) presents

[1] A 75% merging fraction has been used instead of the default 50%.

the measured integrated jet shapes, $\Psi(r/R)$, for jets with $37 < P_T^{\rm jet} < 45$ GeV, compared to HERWIG, PYTHIA-Tune A, PYTHIA and PYTHIA-(no MPI) predictions. In addition, Figure 7(right) shows, for a fixed radius $r_0 = 0.3$, the average fraction of the jet transverse momentum outside $r = r_0$, $1 - \Psi(r_0/R)$, as a function of $P_T^{\rm jet}$ where the points are located at the weighted mean in each $P_T^{\rm jet}$ range. The measurements show that the fraction of jet transverse momentum at a given fixed r_0/R increases ($1 - \Psi(r_0/R)$ decreases) with $P_T^{\rm jet}$, indicating that the jets become narrower as $P_T^{\rm jet}$ increases. PYTHIA with default parameters produces jets systematically narrower than the data in the whole region in $P_T^{\rm jet}$. The contribution from secondary parton interactions between remnants to the predicted jet shapes (shown by the difference between PYTHIA and PYTHIA-(no MPI) predictions) is relatively small and decreases as $P_T^{\rm jet}$ increases. PYTHIA-Tune A predictions describe all of the data well. HERWIG predictions describe the measured jet shapes well for $P_T^{\rm jet} > 55$ GeV but produces jets that are too narrow at lower $P_T^{\rm jet}$. Figure 8(left) shows the

Figure 8: *The measured integrated jet shape compared to the predictions of PYTHIA-Tune A and the separated contributions from quark- and gluon-jets.*

measured integrated jet shapes, $\Psi(r/R)$, for jets with $37 < P_T^{\rm jet} < 45$ GeV, compared to PYTHIA-Tune A and the predictions for quark- and gluon-jets[2] separately. Figure 8(right) shows the measured $1 - \Psi(r_0/R)$, $r_0 = 0.3$, as a function of $P_T^{\rm jet}$. The Monte Carlo predictions indicate that the measured jet shapes are dominated by contributions from gluon-initiated jets at low $P_T^{\rm jet}$ while contributions from quark-initiated jets become important at high $P_T^{\rm jet}$.

[2]Each hadron-level jet from PYTHIA is classified as a quark- or gluon-jet by matching ($y - \phi$ plane) its directions with that of one of the outgoing partons from the hard interaction.

This can be explained in terms of the different partonic contents in the proton and antiproton in the low- and high-$P_T^{\rm jet}$ regions, since the mixture of gluon- and quark-jet in the final state partially reflects the nature of the incoming partons that participate in the hard interaction. For a given type of parton-jet in the Monte Carlo (quark- or gluon-jet), the observed trend with $P_T^{\rm jet}$ shows the running of the strong coupling constant, $\alpha_s(P_T^{\rm jet})$. Jet shape measurements thus introduce strong constrains on phenomenological models describing soft-gluon radiation and the underlying event in hadron-hadron interactions. Similar studies with b-tagged jets will be necessary to test our knowledge of b-quark jet fragmentation processes in hadronic interactions, which is essential for future precise Top and Higgs measurements.

5 $\Delta\phi_{\rm dijet}$ Decorrelations

The D0 experiment has employed the dijet sample to study azimuthal decorrelations, $\Delta\phi_{\rm dijet}$, between the two leading jets. The normalized cross section:

$$\frac{1}{\sigma_{\rm dijet}}\frac{d\sigma}{d\Delta\phi_{\rm dijet}} \tag{3}$$

is sensitive to the spectrum of the gluon radiation in the event. The measurements has been performed in different regions of the leading jet $P_T^{\rm jet}$ starting at $P_T^{\rm jet} > 75$ GeV and the second jet is requied to have at least $P_T^{\rm jet} > 40$ GeV.

Figure 9: *Measured azimuthal decorrelations in dijet production for central jets compared to pQCD predictions in different regions of $P_T^{\rm jet}$ of the leading jet.*

Figure 9 shows the measured cross section compared to LO and NLO predictions from NLOJET++ program [8]. The LO predictions, with at most

three partons in the final state, is limited to $\Delta\phi_{\rm dijet} > 2\pi/3$, for which the three partons define a *Mercedes-star* topology. It presents a prominent peak at $\Delta\phi_{\rm dijet} = \phi$ corresponding to the soft limit for which the third parton is collinear to the direction of the two leading partons. The NLO predictions, with four partons in the final state, describes the measured $\Delta\phi_{\rm dijet}$ distribution except at very high and very low values of $\Delta\phi_{\rm dijet}$ where additional soft constributions, corresponding to a resummed calculation, are necessary. A reasonable approximation to such calculations is provided by parton shower Monte Carlo programs.

Figure 10: *Measured azimuthal decorrelations in dijet production for central jets compared to PYTHIA and HERWIG predictions in different regions of leading* $P_T^{\rm jet}$.

Figure 10 presents the measured cross section compared to PYTHIA-Tune A, PYTHIA and HERWIG predictions in different regions of $P_T^{\rm jet}$. PYTHIA with default parameters underestimates the gluon radiation at large angles. PYTHIA-Tune A predictions, which include an enhanced contribution from initial-state soft gluon radiation and secondary parton interactions, describe the azimuthal distribution. HERWIG also describes the data although tends to produce less radiation than PYTHIA-Tune A close to the direction of the leading jets.

6 Summary and Conclusions

Both CDF and DØ experiments have carried out measurements of the inclusive jet production cross section in Run II at the Tevatron using different jet algorithms. The measurements are in agreement with pQCD NLO predictions. Dedicated studies of the underlying event, jet shapes and azimuthal decorrela-

tions in dijet final states allowed to establish the validity of the Monte Carlo models used to describe the soft-gluon contributions in the final state.

7 Acknowledgements

I thank the organizers for their kind invitation to the conference and for the exciting program of talks and discussions they made possible.

References

1. Stephen D. Ellis, Davision E. Soper, Phys.Rev. **D 48** 3160-3166 (1993).
2. W.T. Giele, E.W.N. Glover, D.A. Kosower, Nucl. Phys.**B 403** 633 (1993).
3. J. Pumplin et al., JHEP **0207** 012 (2002).
4. G. C. Blazey, et al., hep-ex/0005012.
   S.D. Ellis, J. Huston and M. Toennesmann, hep-ph/0111434.
5. H.-U. Bengtsson and T. Sjöstrand, Comp. Phys. Comm. **46** 43 (1987).
6. G. Marchesini et al., Comp. Phys. Comm. **67** 465 (1992).
7. D. Acosta et al., CDF Collaboration, Phys. Rev. **D65**, 092002 (2002).
8. Zoltán Nagy, Zoltán Trócsányi, Phys.Rev.Lett. **79** 3604 (1997).

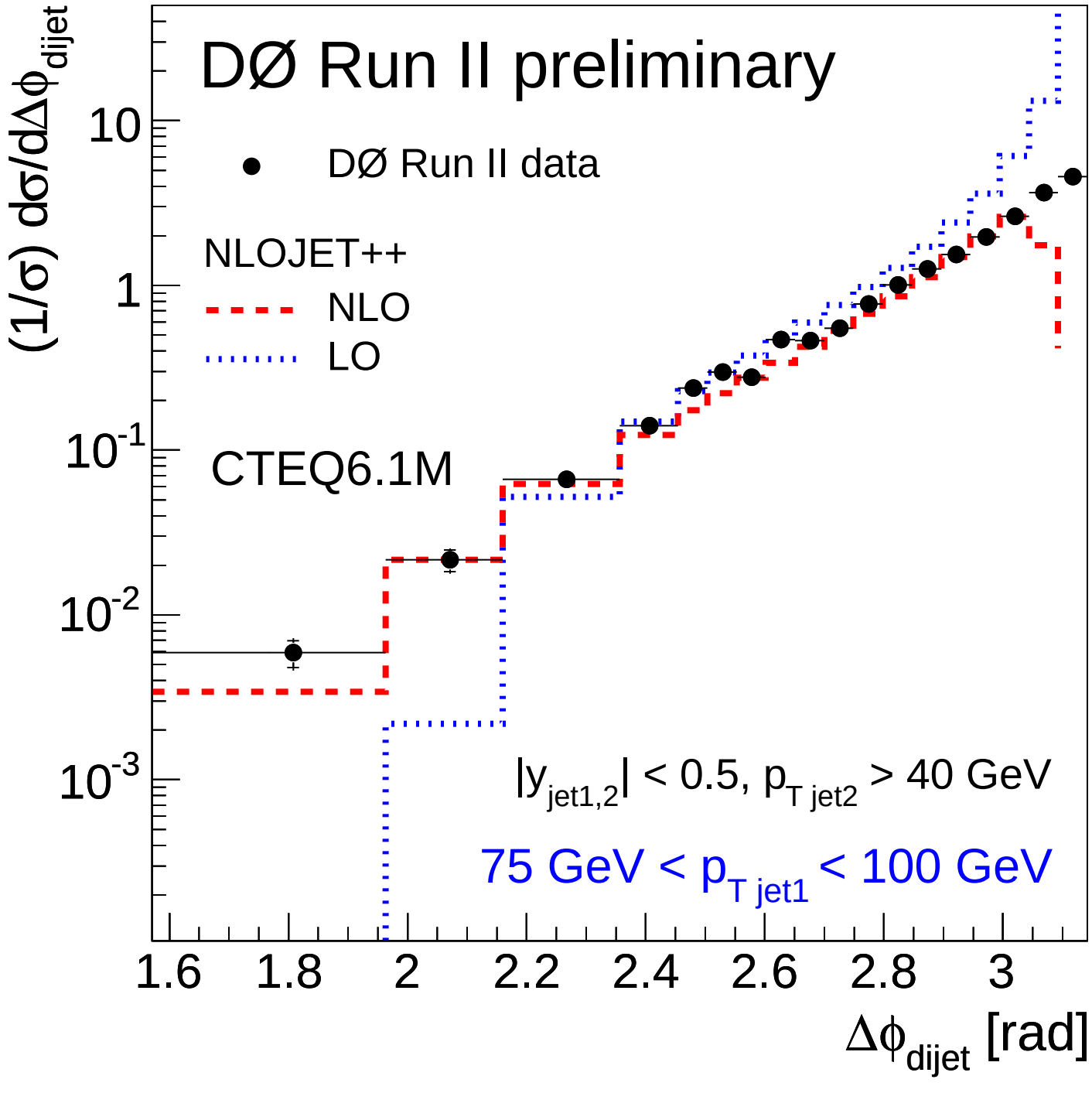
DØ Run II preliminary
DØ Run II data
NLOJET++
NLO
LO
CTEQ6.1M
$|y_{jet1,2}| < 0.5$, $p_{T\ jet2} > 40$ GeV
75 GeV < $p_{T\ jet1}$ < 100 GeV
$(1/\sigma)\ d\sigma/d\Delta\phi_{dijet}$
$\Delta\phi_{dijet}$ [rad]
10
1
10^{-1}
10^{-2}
10^{-3}
1.6
1.8
2
2.2
2.4
2.6
2.8
3

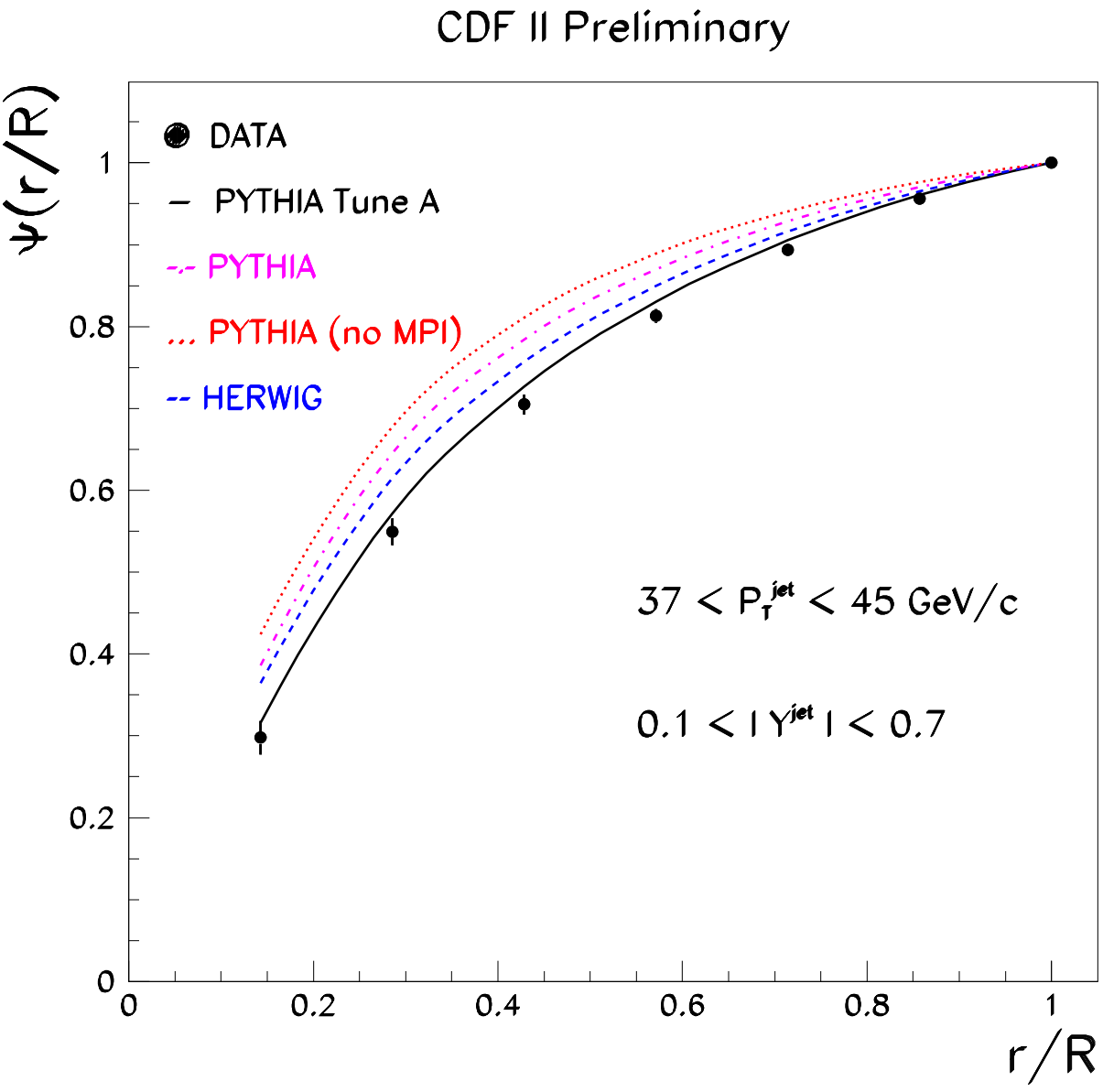
CDF II Preliminary
ψ(r/R)
DATA
PYTHIA Tune A
PYTHIA
PYTHIA (no MPI)
HERWIG
37 < P_T^jet < 45 GeV/c
0.1 < | Y^jet | < 0.7
0
0.2
0.4
0.6
0.8
1
r/R

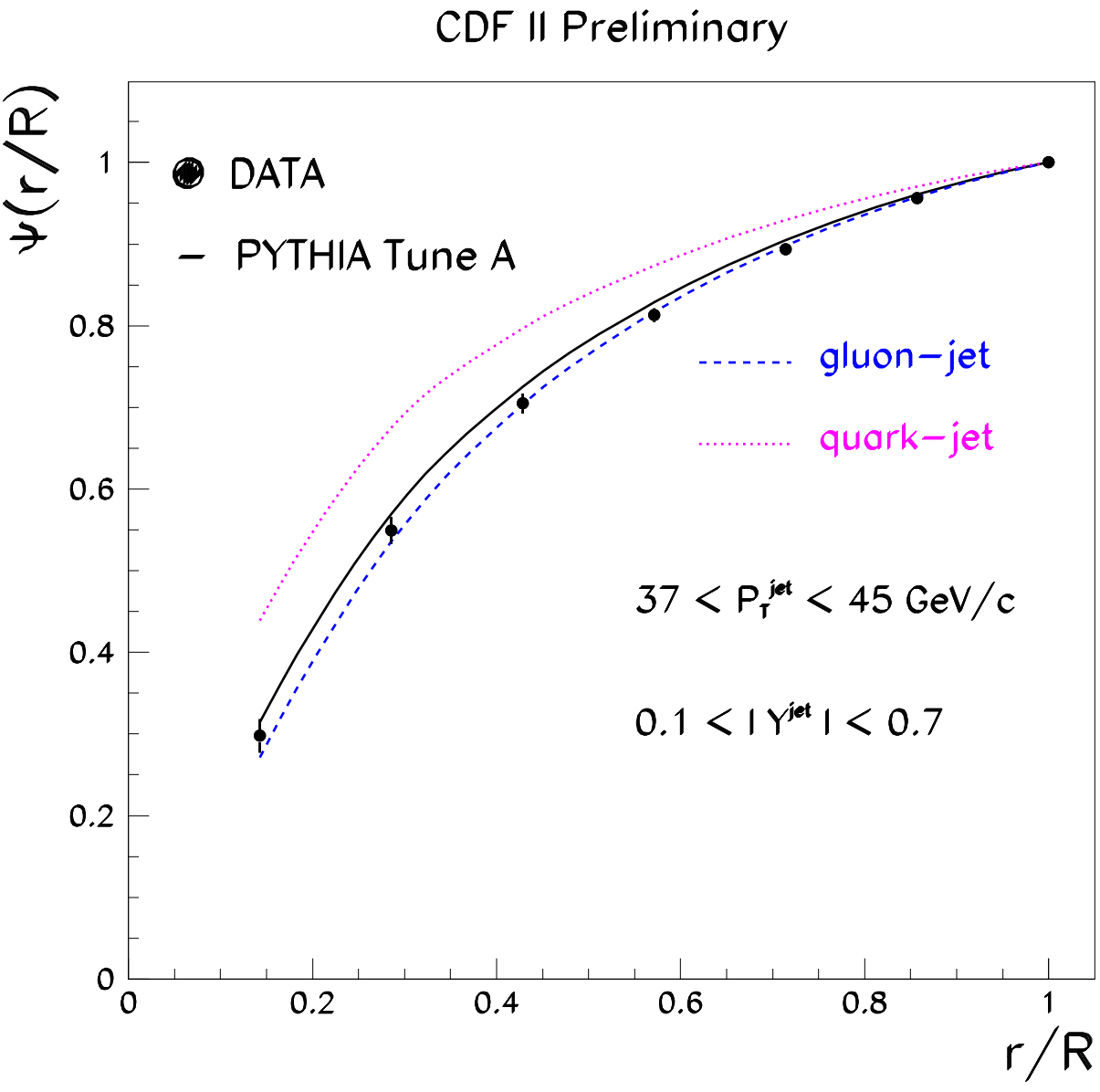
CDF II Preliminary
ψ(r/R)
DATA
PYTHIA Tune A
gluon−jet
quark−jet
37 < P_T^jet < 45 GeV/c
0.1 < | Y^jet | < 0.7
r/R
0
0.2
0.4
0.6
0.8
1

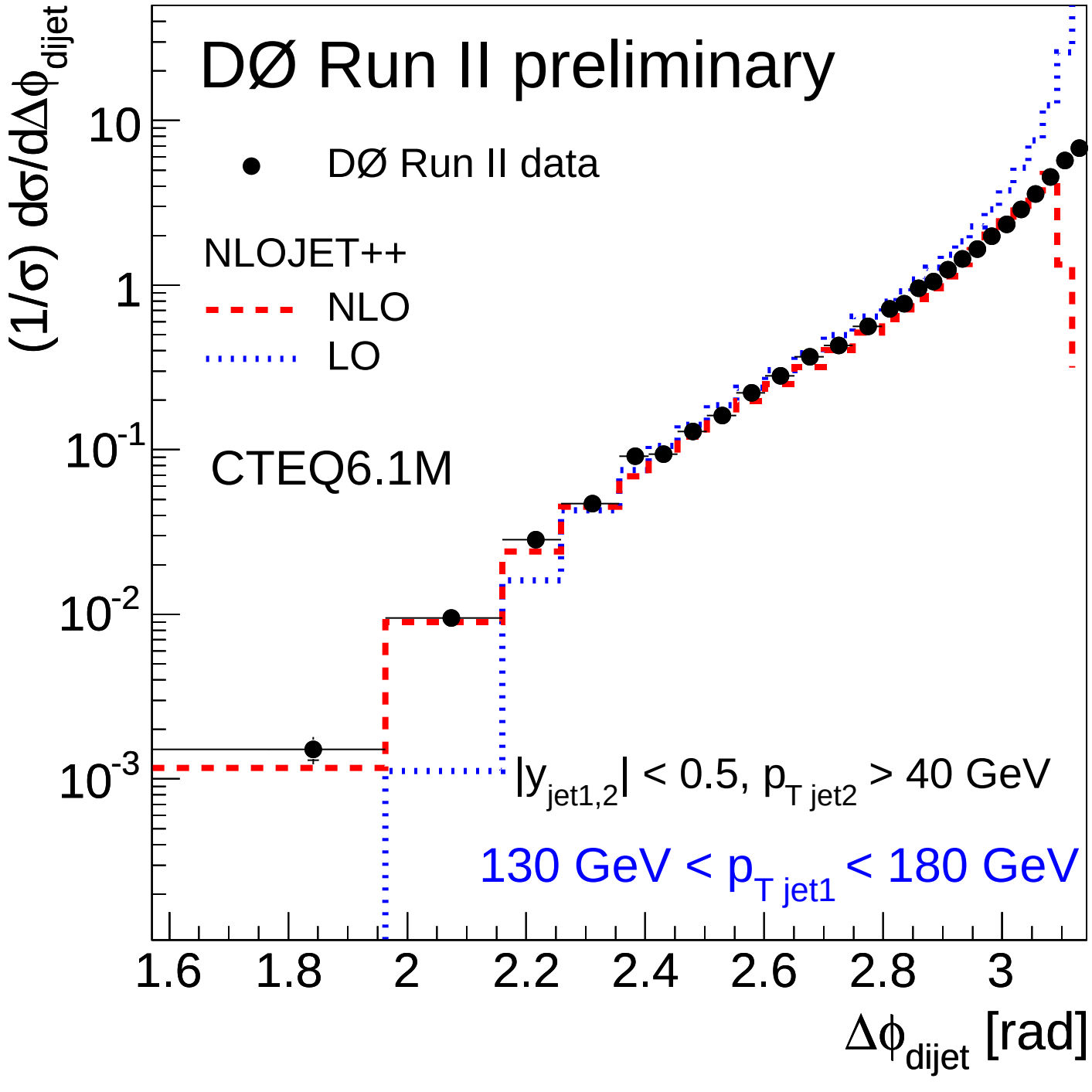
DØ Run II preliminary
DØ Run II data
NLOJET++
NLO
LO
CTEQ6.1M
$|y_{jet1,2}| < 0.5$, $p_{T\,jet2} > 40$ GeV
130 GeV < $p_{T\,jet1}$ < 180 GeV
$(1/\sigma)\ d\sigma/d\Delta\phi_{dijet}$
$\Delta\phi_{dijet}$ [rad]
10
1
10^{-1}
10^{-2}
10^{-3}
1.6
1.8
2
2.2
2.4
2.6
2.8
3

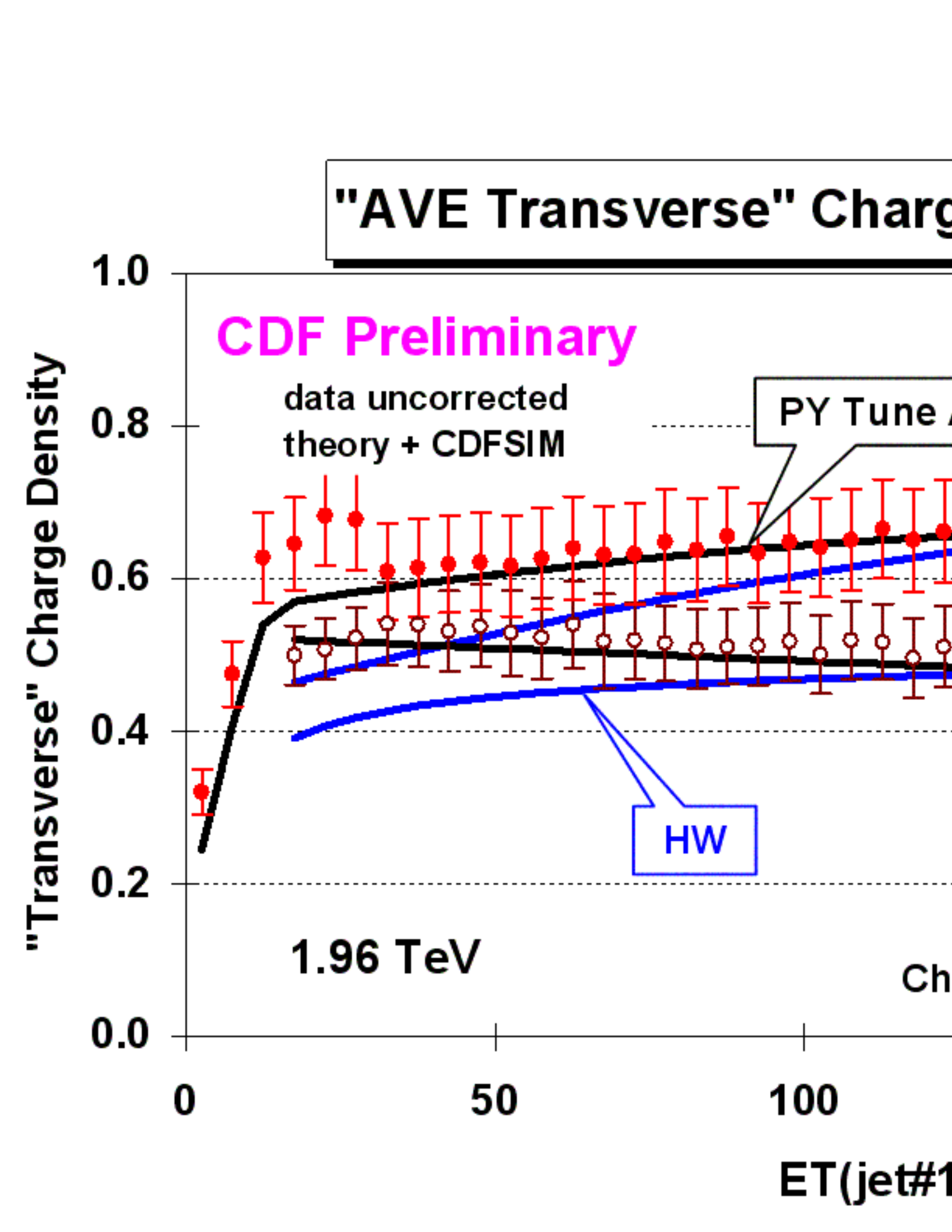
"AVE Transverse" Charg
CDF Preliminary
data uncorrected
theory + CDFSIM
PY Tune
HW
1.96 TeV
"Transverse" Charge Density
1.0
0.8
0.6
0.4
0.2
0.0
0
50
100
ET(jet#1

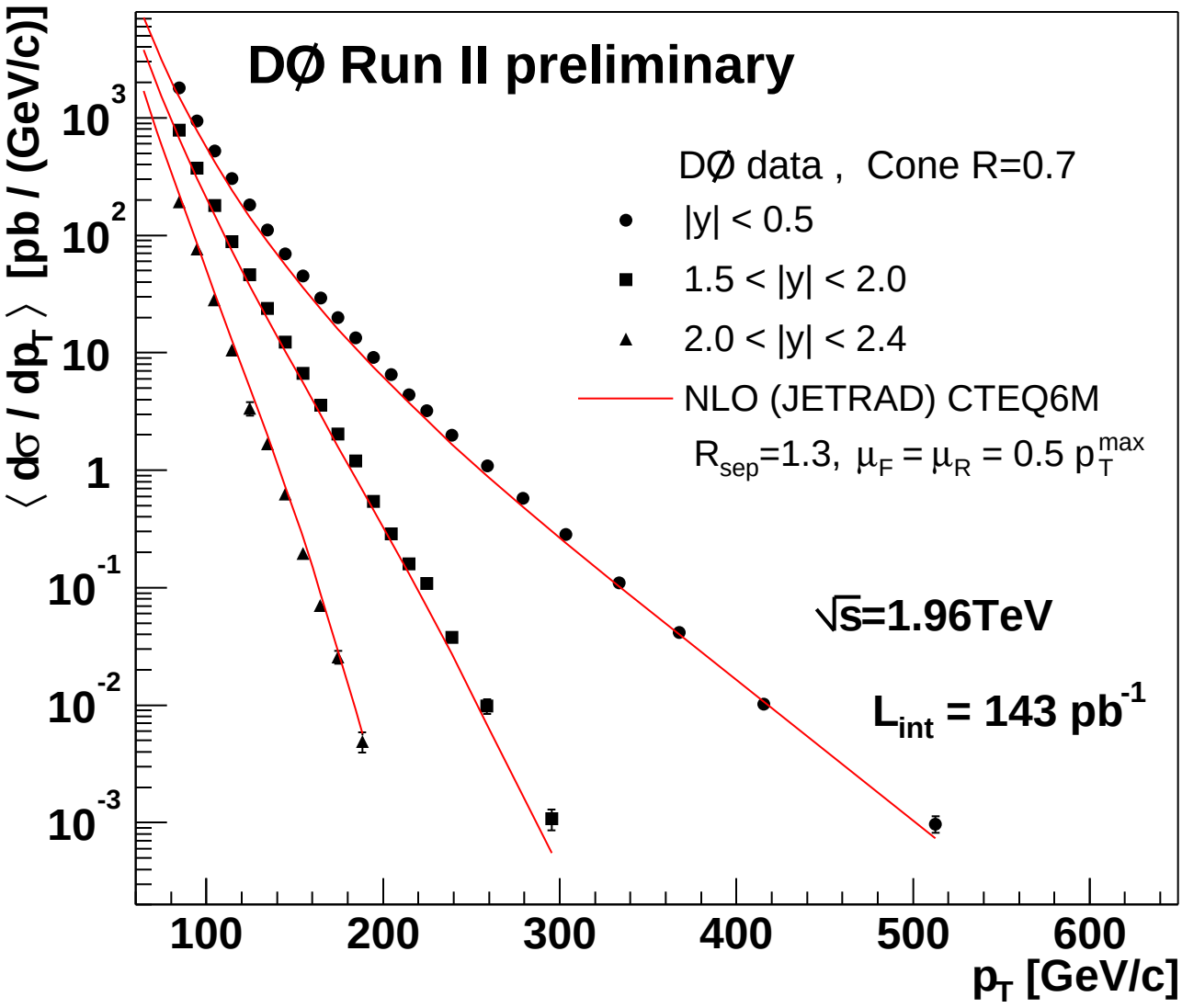
DØ Run II preliminary
DØ data , Cone R=0.7
|y| < 0.5
1.5 < |y| < 2.0
2.0 < |y| < 2.4
NLO (JETRAD) CTEQ6M
R_sep=1.3, μ_F = μ_R = 0.5 p_T^max
√s=1.96TeV
L_int = 143 pb^-1
⟨ dσ / dp_T ⟩ [pb / (GeV/c)]
p_T [GeV/c]
10^3
10^2
10
1
10^-1
10^-2
10^-3
100
200
300
400
500
600

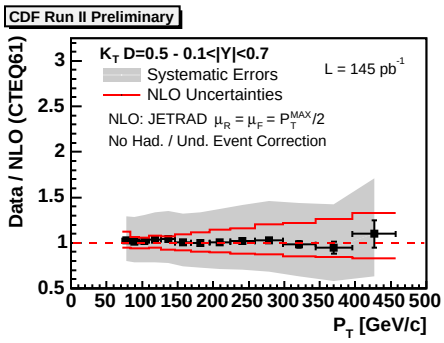
CDF Run II Preliminary
K_T D=0.5 - 0.1<|Y|<0.7
L = 145 pb^{-1}
Systematic Errors
NLO Uncertainties
NLO: JETRAD $\mu_R = \mu_F = P_T^{MAX}/2$
No Had. / Und. Event Correction
Data / NLO (CTEQ61)
3
2.5
2
1.5
1
0.5
0
50
100
150
200
250
300
350
400
450
500
P_T [GeV/c]

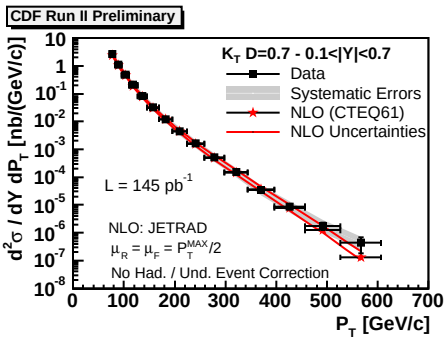
CDF Run II Preliminary
K_T D=0.7 - 0.1<|Y|<0.7
Data
Systematic Errors
NLO (CTEQ61)
NLO Uncertainties
L = 145 pb^{-1}
NLO: JETRAD
$\mu_R = \mu_F = P_T^{MAX}/2$
No Had. / Und. Event Correction
$d^2\sigma$ / dY dP$_T$ [nb/(GeV/c)]
P$_T$ [GeV/c]

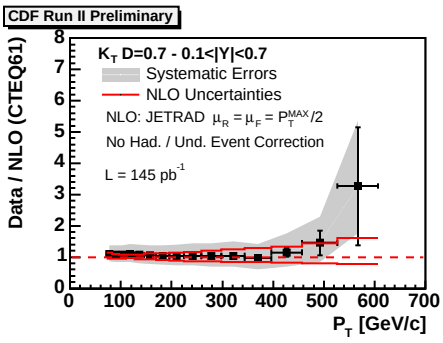
CDF Run II Preliminary
K_T D=0.7 - 0.1<|Y|<0.7
Systematic Errors
NLO Uncertainties
NLO: JETRAD $\mu_R = \mu_F = P_T^{MAX}/2$
No Had. / Und. Event Correction
L = 145 pb^{-1}
Data / NLO (CTEQ61)
P_T [GeV/c]
0
1
2
3
4
5
6
7
8
0
100
200
300
400
500
600
700

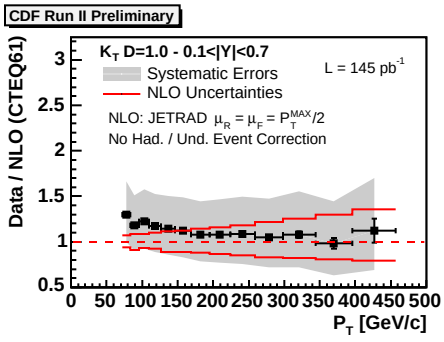
CDF Run II Preliminary
K_T D=1.0 - 0.1<|Y|<0.7
L = 145 pb^{-1}
Systematic Errors
NLO Uncertainties
NLO: JETRAD $\mu_R = \mu_F = P_T^{MAX}/2$
No Had. / Und. Event Correction
Data / NLO (CTEQ61)
0.5
1
1.5
2
2.5
3
0 50 100 150 200 250 300 350 400 450 500
P_T [GeV/c]

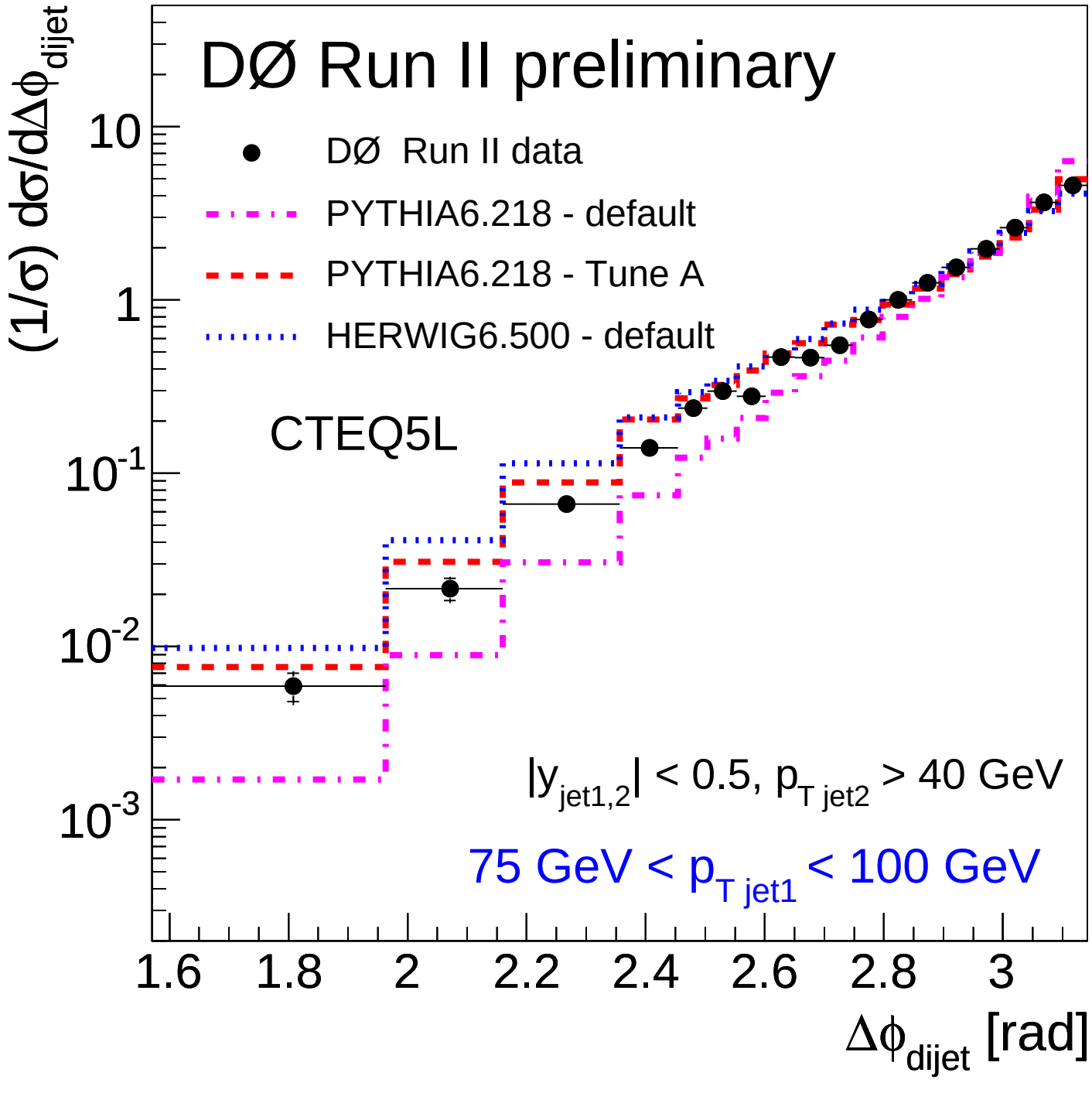
DØ Run II preliminary
DØ Run II data
PYTHIA6.218 - default
PYTHIA6.218 - Tune A
HERWIG6.500 - default
CTEQ5L
$|y_{jet1,2}| < 0.5$, $p_{T\ jet2} > 40$ GeV
75 GeV < $p_{T\ jet1}$ < 100 GeV
$(1/\sigma)\ d\sigma/d\Delta\phi_{dijet}$
$\Delta\phi_{dijet}$ [rad]
10
1
10^{-1}
10^{-2}
10^{-3}
1.6
1.8
2
2.2
2.4
2.6
2.8
3

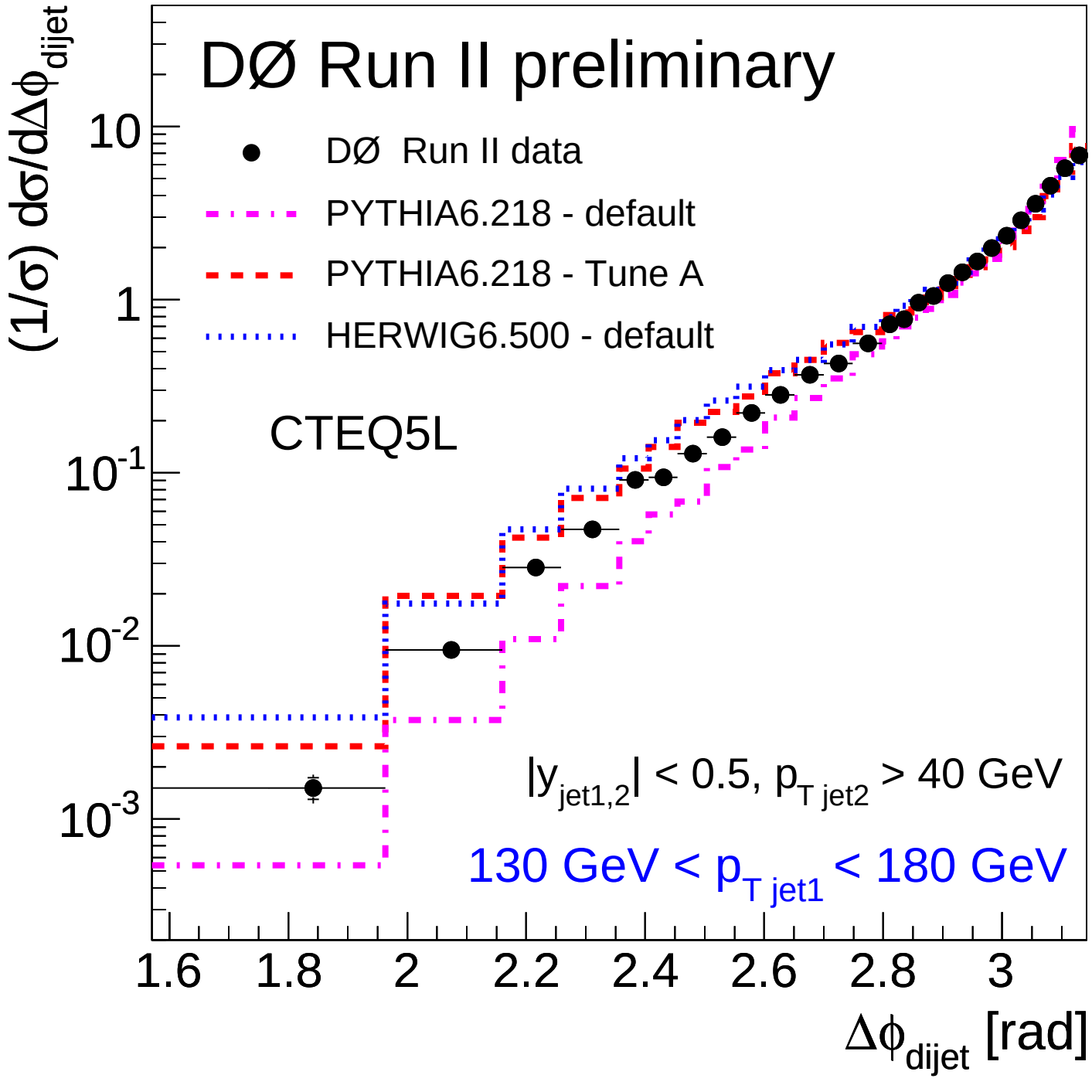
DØ Run II preliminary
DØ Run II data
PYTHIA6.218 - default
PYTHIA6.218 - Tune A
HERWIG6.500 - default
CTEQ5L
$|y_{jet1,2}| < 0.5$, $p_{T\,jet2} > 40$ GeV
130 GeV < $p_{T\,jet1}$ < 180 GeV
$(1/\sigma)\, d\sigma/d\Delta\phi_{dijet}$
$\Delta\phi_{dijet}$ [rad]
10
1
10^{-1}
10^{-2}
10^{-3}
1.6
1.8
2
2.2
2.4
2.6
2.8
3

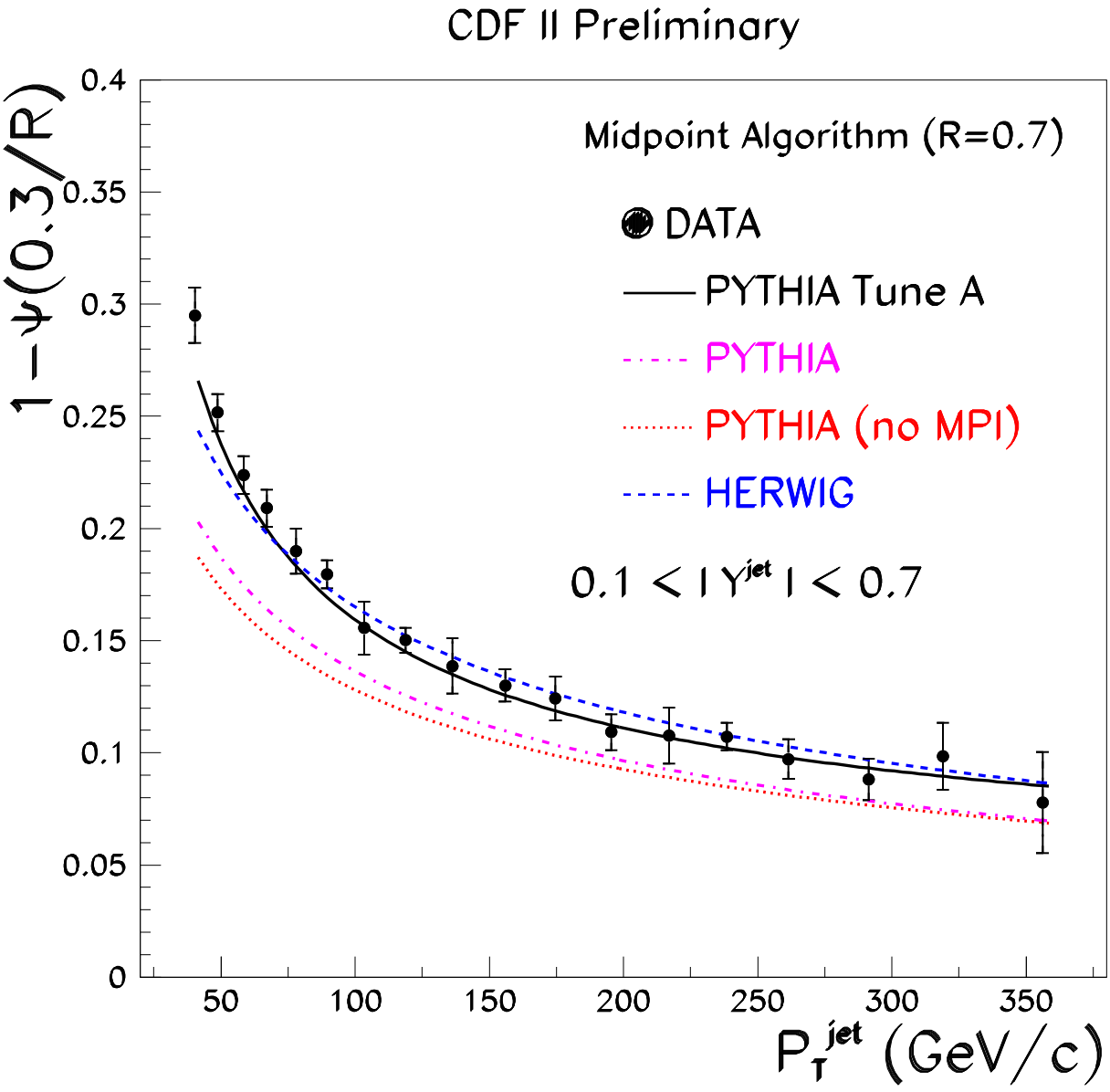
CDF II Preliminary
Midpoint Algorithm (R=0.7)
DATA
PYTHIA Tune A
PYTHIA
PYTHIA (no MPI)
HERWIG
0.1 < | Y^jet | < 0.7
1−Ψ(0.3/R)
P_T^jet (GeV/c)
0
0.05
0.1
0.15
0.2
0.25
0.3
0.35
0.4
50
100
150
200
250
300
350

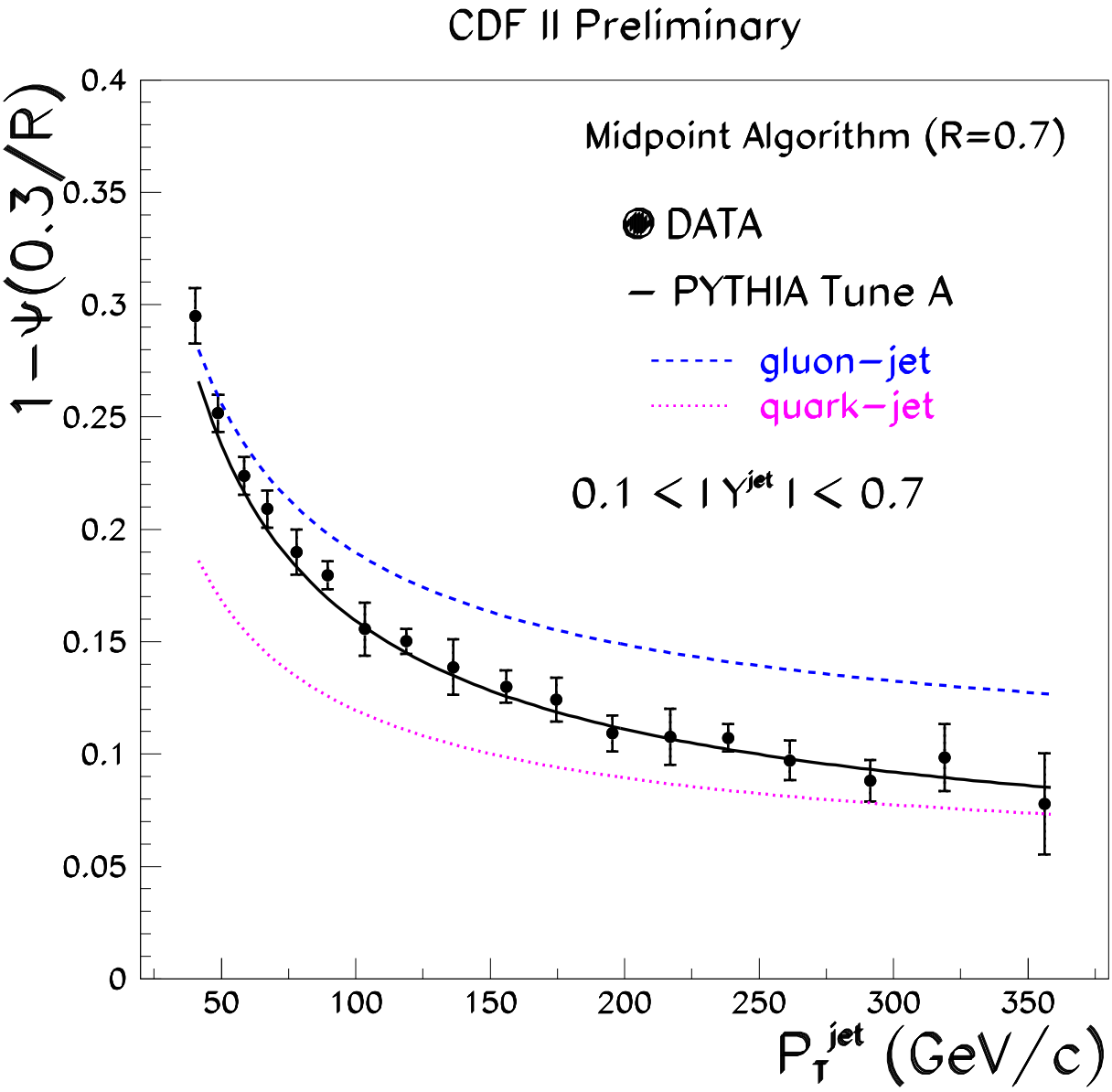
CDF II Preliminary
Midpoint Algorithm (R=0.7)
DATA
PYTHIA Tune A
gluon−jet
quark−jet
0.1 < | Y^jet | < 0.7
1−ψ(0.3/R)
P_T^jet (GeV/c)
0
0.05
0.1
0.15
0.2
0.25
0.3
0.35
0.4
50
100
150
200
250
300
350

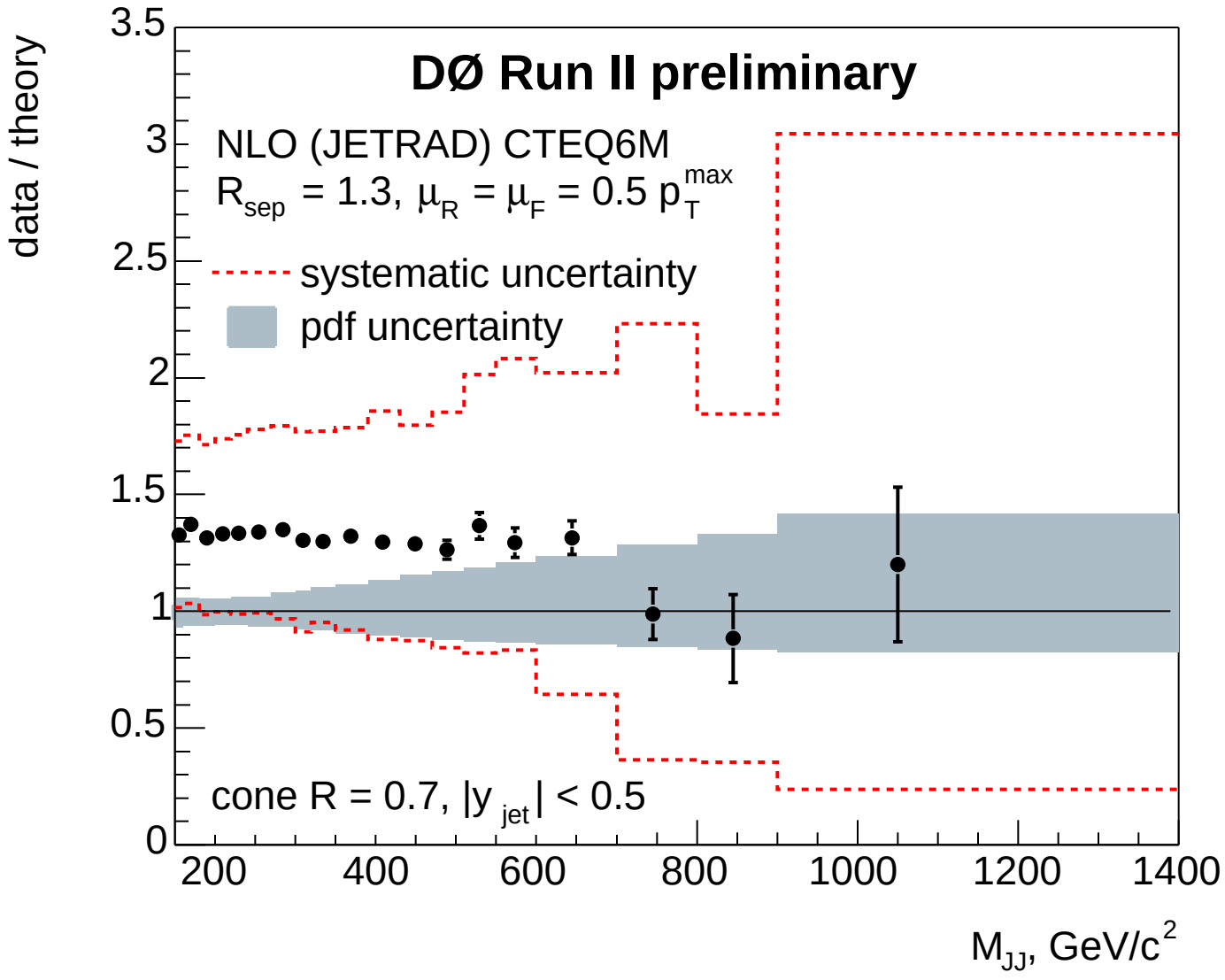
DØ Run II preliminary
NLO (JETRAD) CTEQ6M
R_{sep} = 1.3, $\mu_R = \mu_F = 0.5\ p_T^{max}$
systematic uncertainty
pdf uncertainty
cone R = 0.7, $|y_{jet}| < 0.5$
data / theory
M_{JJ}, GeV/c^2
0
0.5
1
1.5
2
2.5
3
3.5
200
400
600
800
1000
1200
1400

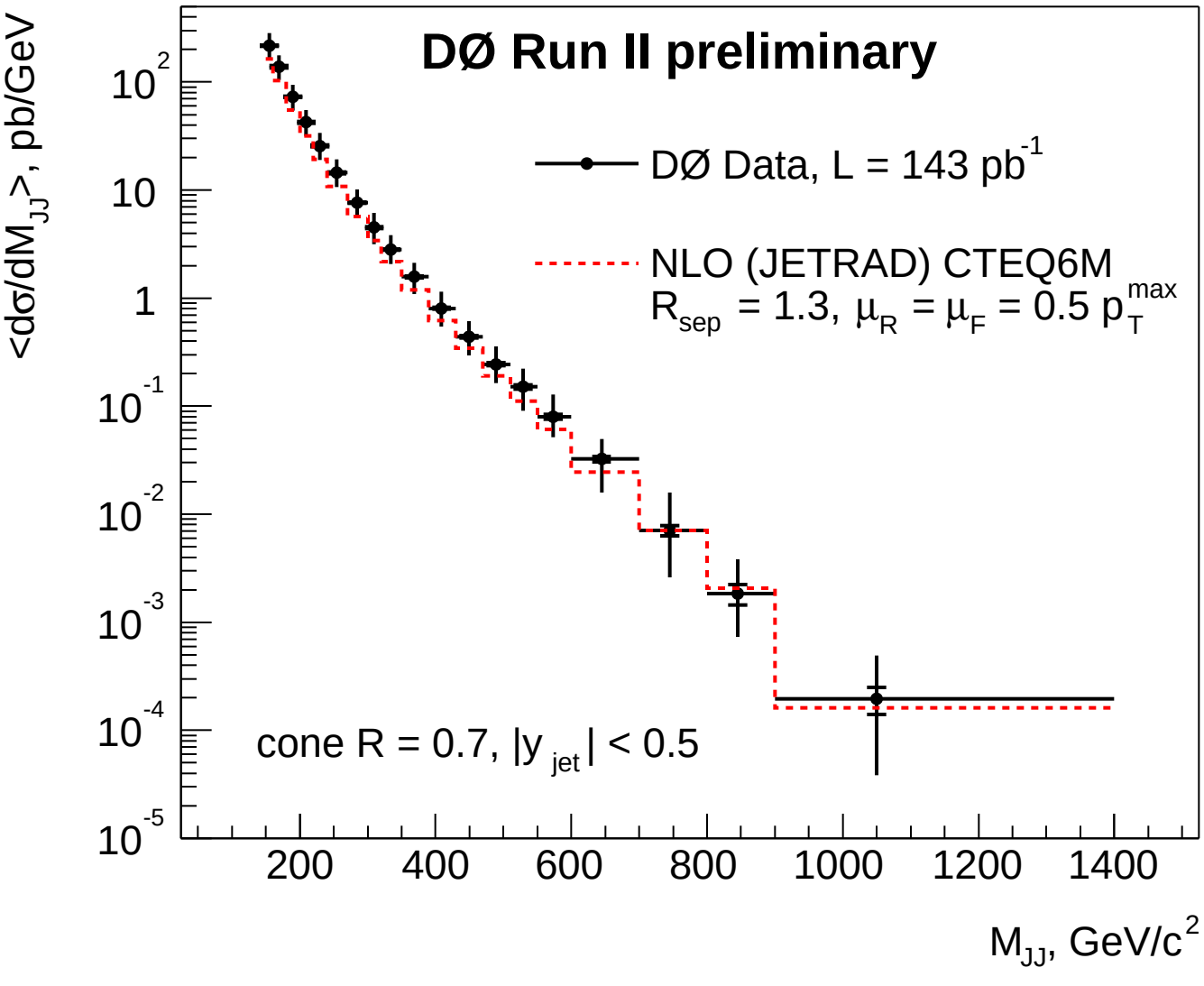
DØ Run II preliminary
DØ Data, L = 143 pb-1
NLO (JETRAD) CTEQ6M
Rsep = 1.3, μR = μF = 0.5 pTmax
cone R = 0.7, |y jet| < 0.5
<dσ/dMJJ>, pb/GeV
MJJ, GeV/c2
10^2
10
1
10^-1
10^-2
10^-3
10^-4
10^-5
200
400
600
800
1000
1200
1400

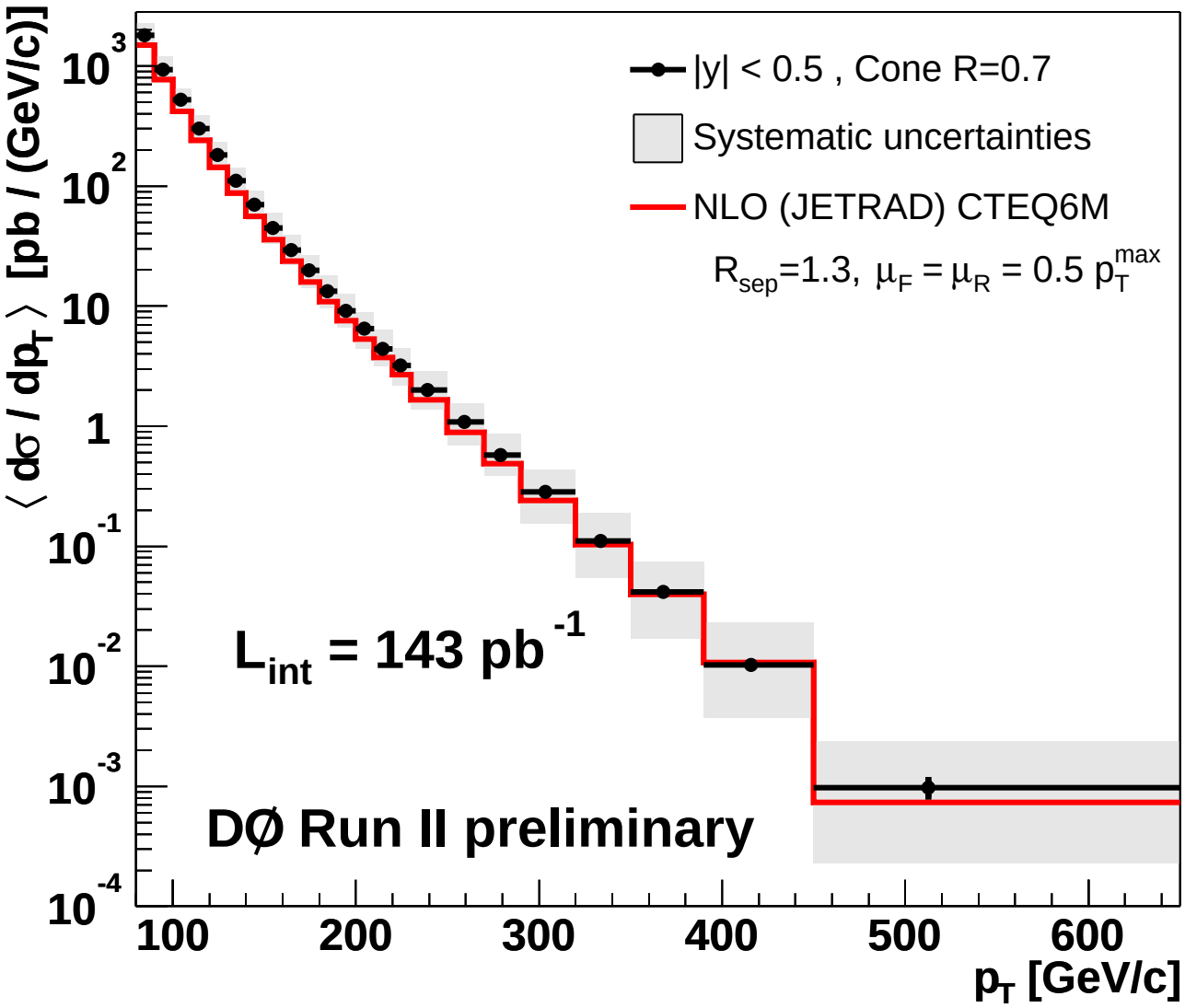
⟨ dσ / dp_T ⟩ [pb / (GeV/c)]
10^3
10^2
10
1
10^-1
10^-2
10^-3
10^-4
100
200
300
400
500
600
p_T [GeV/c]
|y| < 0.5 , Cone R=0.7
Systematic uncertainties
NLO (JETRAD) CTEQ6M
R_sep=1.3, μ_F = μ_R = 0.5 p_T^max
L_int = 143 pb^-1
DØ Run II preliminary

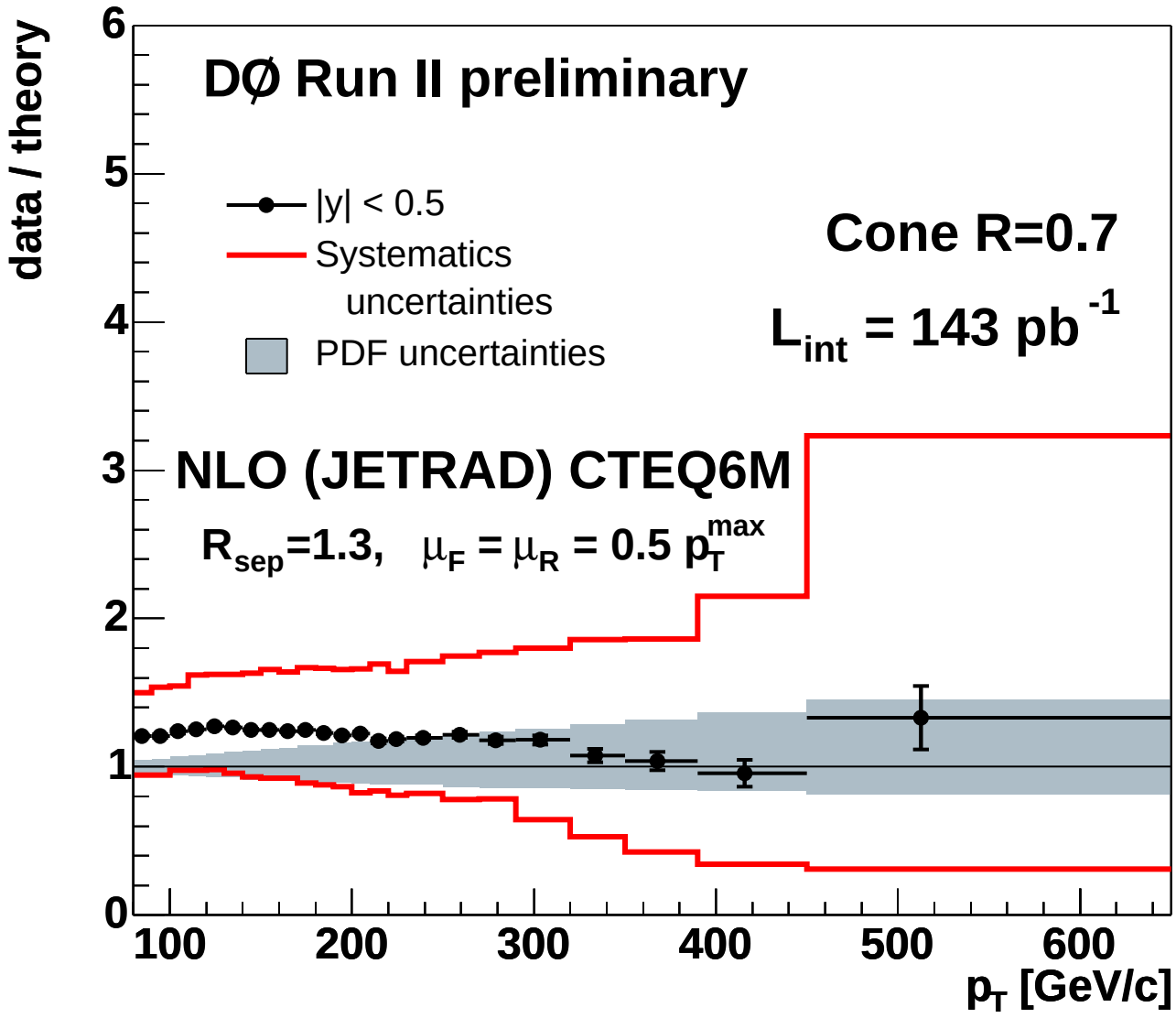
DØ Run II preliminary
|y| < 0.5
Systematics uncertainties
PDF uncertainties
Cone R=0.7
L_int = 143 pb^-1
NLO (JETRAD) CTEQ6M
R_sep=1.3, μ_F = μ_R = 0.5 p_T^max
data / theory
p_T [GeV/c]
0
1
2
3
4
5
6
100
200
300
400
500
600

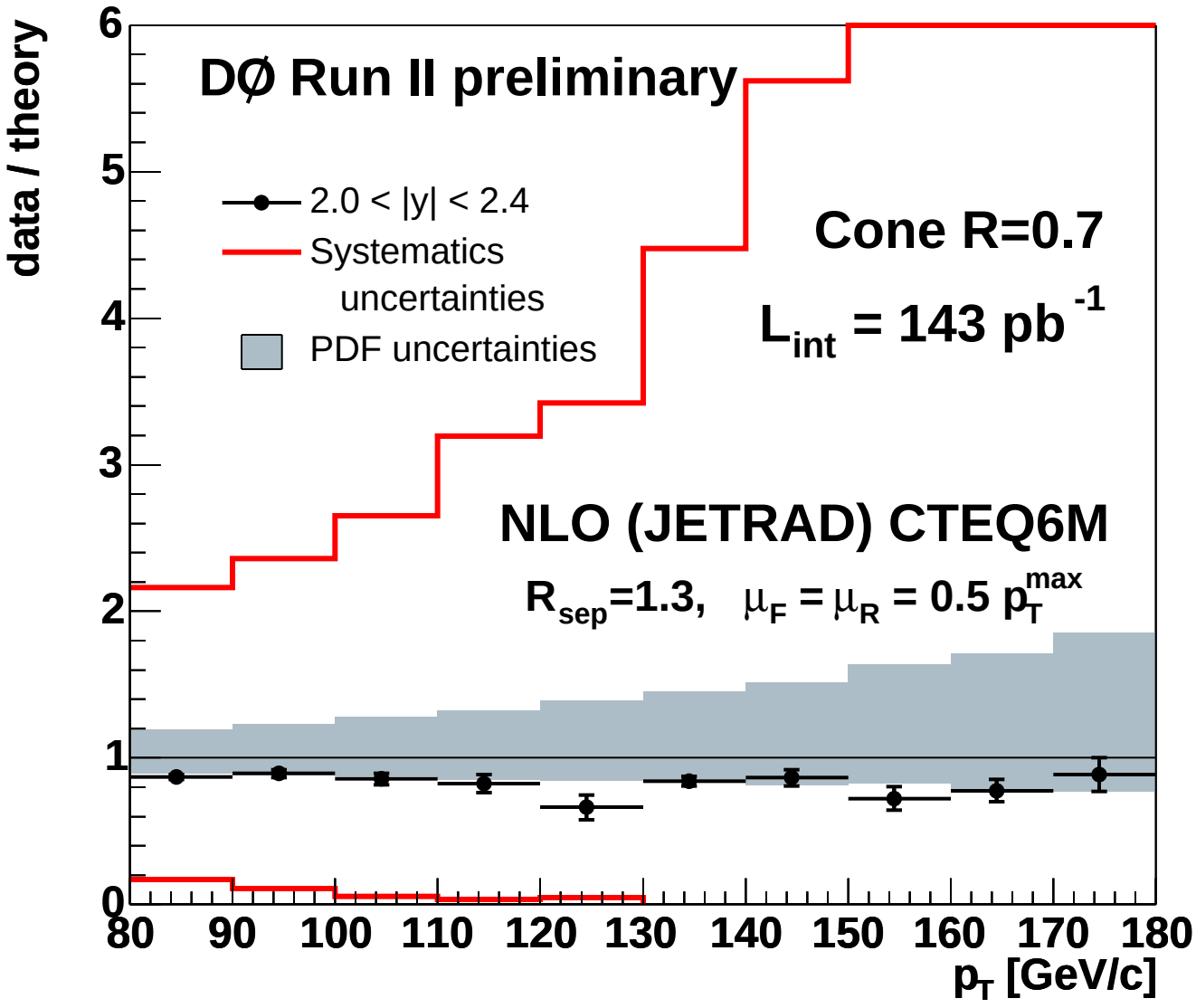
DØ Run II preliminary
2.0 < |y| < 2.4
Systematics uncertainties
PDF uncertainties
Cone R=0.7
L_int = 143 pb^-1
NLO (JETRAD) CTEQ6M
R_sep=1.3, μ_F = μ_R = 0.5 p_T^max
data / theory
p_T [GeV/c]
0
1
2
3
4
5
6
80
90
100
110
120
130
140
150
160
170
180